Cell. Mol. Biol. (ISSN: 1165-158X)

Journal Homepage: www.cellmolbiol.org

Cellular and Molecular Biology

Original Article

MiR-4319 targets tuftelin 1 to reduce malignancy of cervical cancer cells

Lijun Zheng[1,#], Qiongzhen Ren[2,#], Weipei Zhu[2], Xiaomin Tao[2], Liangsheng Guo[2,*]

[1] *Department of ultrasound, The Second Affiliated Hospital of Soochow University, Suzhou, Jiangsu, China*
[2] *Department of Obstetrics and Gynaecology, The Second Affiliated Hospital of Soochow University, Suzhou, Jiangsu, China*

Article Info

Article history:

Received: January 09, 2024
Accepted: February 13, 2024
Published: March 31, 2024

Use your device to scan and read the article online

Abstract

Cervical cancer (CC) is the most common malignant tumor of female reproductive system. MiR-4319 has been identified as an anti-oncogene in various cancers. In the present study, role of miR-4319 in CC was identified. Colony formation, flow cytometer, wound healing, and transwell assays were used to detect CC cell proliferation, apoptosis, migration, and invasion. The expression of miR-4319 was decreased in clinical CC tissues and CC cell lines. Upregulation of miR-4319 suppressed cell viability, proliferation, migration, and invasion, and induced cell apoptosis in CC cells. Moreover, tuftelin 1 (TUFT1) was verified as a direct target of miR-4319, as confirmed by dual-luciferase reporter assay. Additionally, TUFT1 expression was remarkably increased in clinical CC tissues and CC cell lines and was negatively associated with miR-4319 expression. Furthermore, overexpression of TUFT1 partially restored the effects of miR-4319 mimic on cell viability, proliferation, migration, invasion, and cell apoptosis in CC cells. To conclude, miR-4319 played an anti-cancer role in the occurrence and development of CC, which might be achieved by targeting TUFT1.

Keywords: Cervical cancer, MicroRNA-4319, Proliferation, Migration, Tuftelin 1.

1. Introduction

Cervical cancer (CC) is one of the most common malignant tumors in women, which occurs in the cervix and vagina (1). According to worldwide statistics, there are about 500, 000 new cases of CC every year, accounting for 5% of all new cancer cases, of which more than 80% are in developing countries (2, 3). Despite the increasing awareness of cancer prevention and treatment in recent years, and the popularity of related vaccines, the incidence rate of CC is still rising, and the age of audience becomes younger and younger (4). A number of studies have shown that persistent high-risk human papilloma virus (HPV) infection is a relatively clear risk factor for CC. In women's lives, cervical HPV infection is quite common, The genital tract infection rate of HPV is more than 75%, but most of them can subside by themselves (5, 6). The main current treatments for CC are surgery, radiotherapy, chemotherapy and other adjuvant therapy (7). It is worth emphasizing that the early symptoms of CC are not obvious, some patients are in advanced stage at the time of diagnosis, and lose the best opportunity for treatment, which seriously threatens the health and quality of women's lives (8). As the disease progresses, the following manifestations including vaginal bleeding, discharge of vaginal fluid, frequent urination, urgent urination, constipation, lower limb swelling and pain, etc may appear (9). Therefore, it is necessary to explore the potential mechanisms of CC for early diagnosis and effective treatment.

MicroRNAs (miRNAs) are a kind of non-coding single-stranded RNA molecule with about 18-25 nucleotides in length (10). MiRNAs cause degradation or translation inhibition of target gene mRNA through specifically pairing with 3'-UTR region of target gene mRNA, further regulating the expression of target genes at post-transcriptional level (11). According to statistics, miRNAs regulate at least 30% of human genes and play an important role in the normal development of the body (12). However, the disorder of miRNA expression is also common in many malignant tumors, including CC. For example, miR-21 and miR-155 are significantly over-expressed in CC tissues and may be helpful in the prediction of both HPV-positive and HPV-negative cases of CC (13). MiR-501 is up-regulated, whereas CYLD protein is down-regulated in CC tissues, and down-regulation of miR-501 inhibits proliferation, migration, and invasion, and promotes apoptosis of CC cells via targeting CYLD mediated with NF-κB p65 signaling pathway (14). MiR-1284 is down-expressed in CC tissues and CC cell lines. Up-regulation of miR-1284 suppresses proliferation and invasion, promotes apoptosis of CC cells, and enhances the sensitivity of CC cells to cisplatin achieved by targeting HMGB1 (15). These findings suggest that miRNAs, acting as oncogenes or tumor sup-

* Corresponding author.
E-mail address: gls2135@sina.com (L. Guo).
# These authors contributed equally
Doi: http://dx.doi.org/10.14715/cmb/2024.70.3.8

pressor genes, exhibit essential functions in the occurrence and development of CC.

MiR-4319, a newly identified cancer-related miRNA, is aberrantly expressed and becomes a predictor of patient survival in cancers (16). For instance, miR-4319 is low-expressed in colorectal cancer tissues, and over-expression of miR-4319 markedly reduces proliferation and induces cell cycle distribution of colorectal cancer cells via targeting PLZF (17). Up-regulation of miR-4319 inhibits triple-negative breast cancer (TNBC) initiation and metastasis in vivo and suppresses the self-renewal in TNBC cancer stem cells (CSCs) through targeting E2F2 (18). Moreover, miR-4319 expression is lower in esophageal squamous cell carcinoma (ESCC) cells, and over-expression of miR-4319 represses cell growth and induces cell cycle arrest via regulating NLRC5 (19). However, the possible effects and underlying mechanisms of miR-4319 on CC remained unknown. Therefore, our intention was designed to elucidate the biological impacts and associated mechanisms of miR-4319 on CC cells.

2. Materials and methods

2.1. Tissue samples

The clinical CC tissues and adjacent tissues were obtained from the Second Affiliated Hospital of Soochow University CC patients who underwent surgery at the Second Affiliated Hospital of Soochow University Hospital. No radiotherapy or chemotherapy was performed before the surgery. All fresh tissues surgically resected were immediately stored at -80 °C. The signed written informed consents were obtained from all the participants before the study. This study was approved by the Ethics Committee of our hospital.

2.2. Cell culture and transfection

The human CC cell lines (CaSki, SiHa, HeLa, and C33A) and the cervical epithelial cells (H8) were provided by the American Type Culture Collection (ATCC, Manassas, VA, USA). CaSki and H8 cells were cultured in RPMI-1640 medium. SiHa, HeLa and C33A cells were cultured in Eagle's Minimum Essential Medium (EMEM). All cell mediums were contained with 10% of fetal bovine serum (FBS, Invitrogen, Grand Island, NY) and 1% penicillin-streptomycin (Sigma- Aldrich, St. Louis, MO) in a humidified condition with 5% CO_2 at 37ºC.

GFP-miR-4319 mimic and miRNA mimic-negative control were purchased from Ambion (Austin, TX, USA). Overexpression vector of TUFT1 and the empty vector were obtained from Thermo Fisher Scientific (USA). HeLa and C33A cells were cultured into 6-well plates and transfected with Lipofectamine 2000 Reagent (Invitrogen, USA) according to the manufacturer's protocols. For GFP-miR-4319 mimic, successful adenovirus transfection was evidenced by green fluorescence under fluorescence microscopy (Olympus).

2.3. Cell counting Kit-8 (CCK-8) assay

Following the protocol of CCK-8 assay (Dojindo Laboratories, Kumamoto, Japan), the cell growth ability of transfected HeLa and C33A cells in 96-well plates was assessed at 0, 24, 48, and 72 h, respectively. Spectrophotometer (Thermo Fisher Scientific, Waltham, MA, USA) was utilized to measure the absorbance at 450 nm.

2.4. Colony formation assay

Transfected HeLa and C33A cells (1×10^3/well) were placed in a 6-well plate, and the medium was replaced with fresh culture medium every 2-3 days for 10 days. The colonies were fixed in 10% formaldehyde for 30 min and stained with 0.5% crystal violet for 5 min. The Image-Pro Plus 6.0 (Silver Springs, MD, USA) was used for data analysis.

2.5. Ethynyl deoxyuridine (EdU) incorporation assay

Transfected HeLa and C33A cells (1×10^4/well) were cultured in 96-well plates and transfected for 48 h. Then HeLa and C33A cells were fixed with 4% paraformaldehyde, Triton X-100 was used to permeabilize the nuclear membrane, and HeLa and C33A cells were blocked with goat serum for 1 h. Furthermore, HeLa and C33A cells were stained according to the manufacturer's manual.

2.6. Cell apoptosis by flow cytometry

The apoptosis rate of transfected HeLa and C33A cells was detected by flow cytometry. Transfected HeLa and C33A cells were collected after 48-h transfection. Washed with PBS, FITC-labeled Annexin V and PI (5 μL each) were added to 500 μL of the cell suspension, mixed and incubated at room temperature for 5-15 min in the dark. Then, the rate of apoptosis was detected by flow cytometry. The experiment was repeated for 3 times.

2.7. Wound healing assay

Transfected HeLa and C33A cells at a density with 1 × 105/mL were seeded in a 6-well plate. Then the cultured cells grew to confluence 80%, the wound was made on the surface of the cell with 200 L tip gun heads. After 0 and 48 h respectively, HeLa and C33A cells were observed with an inverted microscope with an inverted microscopy (Tokyo, Japan), and the distance between the wounds was recorded.

2.8. Transwell migration and invasion assays

Transwell migration and invasion assays (Corning Inc.; USA) were performed to determine the migration and invasion capacities of HeLa and C33Acells. For transwell invasion assay, Matrigel (Becton-Dickinson Pharmingen, San Diego, CA, USA), dissolved at 4°C overnight, was diluted with serum-free medium and added to the upper chambers to form a gel for 30 min at 37°C with 5% CO_2. Then for transwell migration and invasion assays, transfected HeLa and C33A cells (1×10^6 cells/well) were seeded into upper chamber with serum-free DMEM medium, and DMEM medium containing 20% FBS was added in the lower chamber. After 48-h incubation, the migration and invasion cells were treated with 70% ethanol, stained with 0.5% crystal violet, and counted by an inverted microscope (Tokyo, Japan).

2.9. RNA extraction and qRT-PCR

TRIzol reagent (Invitrogen, Carlsbad, CA, USA) was utilized to extract the total RNA from clinical CC tissues and cell lines. Through the reverse Transcription Kit (TaKaRa Biotechnology Co., Ltd., Dalian, China), the total RNA was reversely transcribed to complementary deoxyribose nucleic acids (cDNAs). Routine qRT-PCR was implemented using ABI 7300-fast RT PCR system (Applied Biosystems) with SYBR Green PCR Kit (Qiagen) based

on the specifications. Relative expressions of miRNA and mRNA were evaluated by the $2^{-\Delta\Delta Ct}$ method with U6 or β-actin as internal reference. The primer sequences used were listed as below: miR-4319 forward, 5'-CACCCAGAGCAAAGCCAC-3', miR-4319 reverse, 5'-GTGCAGGGTCCGAGGT-3', TUFT1 forward, 5'-TGGTCTGAGCTCGCCATCAGTTTCA-3', TUFT1 reverse, 5'-CCCTGAGGGACCAGCCACATAGAACAGA-3', U6 forward, 5'-CTCGCTTCG GCAGCACA-3', U6 reverse, 5'-AACGCTTCACGAATTTGCGT-3', β-actin forward, 5'-AGAAGGC TGGGGCTCATTTG-3', β-actin reverse, 5'-AGGGGCCATCCACAGTCTTC-3'. Conditions for qRT-PCR were used: 95°C for 10 min, 40 cycles of 95°C for 15 s, and 60°C for 1 min.

2.10. Western blot analysis

The protein of CC cells was lysed in RIPA lysis buffer. After 12, 000 g centrifugation for 15 min at 4°C, the total protein concentrations were determined by BCA protein assay kit (Beyotime, Haimen, China). Equivalent samples were separated using 10% SDS-PAGE and then transferred onto a PVDF membrane for 2 h. Then they were blocked with 5% nonfat skim milk in Tris-Buffered Saline and Tween-20 (TBS-T) buffer at room temperature for 1 h and incubated with the following primary antibodies at 4°C overnight: anti-Bcl-2 (1: 1, 000, ab32124), anti-Bax (1: 1, 000, ab32053), anti-cleaved caspase-3 (1: 1, 000, ab32042), anti-cleaved caspase-9 (1: 1, 000, ab2324), anti-Cox-2 (1: 1, 000, ab15191), anti-MMP-2 (1: 1, 000, ab97779), anti-MMP-9 (1: 1, 000, ab38898), anti-TUFT1 (1: 1, 000, ab184949), anti-β-actin (1: 1, 000, ab8226). After the primary antibodies were washed three times with TBS-T, the second antibody was added and incubated for 2 h at room temperature. Enhanced Chemiluminescence Detection System was carried out to evaluate the protein expressions. β-actin was used as the loading control. All antibodies were purchased from Abcam (Cambridge, MA, USA).

2.11. Dual-luciferase reporter assay

3'-untranslated region (3'-UTR) of TUFT1 was cloned into the pGL3 vector (Promega, Madison, WI, USA), which was identified as wild-type (WT) 3'-UTR. The quick-change site-directed mutagenesis kit (Stratagene, Cedar Creek, USA) was used for site-directed mutagenesis of the miR-4319 binding site in TUFT1 3'-UTR, which was named as mutant (MUT) 3'-UTR. Cells were co-transfected with WT-3'-UTR/MUT-3'-UTR and NC mimic or miR-4319 mimic for 48 h. Dual-luciferase reporter assay system (Promega, Madison, WI, USA) was used for determining luciferase activity.

2.12. Statistical analysis

Statistical analysis was conducted by the Statistical Product and Service Solutions (SPSS) 17.0 (SPSS Inc., Chicago, IL, USA). The Student's t-test was performed to compare inter group differences. Data were presented as mean ± standard deviation (SD). $P< 0.05$ was considered of statistical significance.

3. Results

3.1. MiR-4319 expression is down-regulated in CC tissues and cell lines

To explore the possible effects and underlying mechanisms of miR-4319 on CC, firstly, qRT-PCR assay was performed to evaluate the expression of miR-4319 in clinical CC tissues and cell lines. The data of Figure 1A showed that miR-4319 expression was significantly down-regulated in CC tissues compared with that in normal tissues. Besides, as expected, the expression of miR-4319 was also decreased in CC cells (especially in HeLa and C33A cells) relative to that in H8 cells (Figure 1B). To further investigate the functional role of miR-4319 in CC cells, miR-4319 mimic and NC mimic were transfected into HeLa and C33A cells, and transfection efficiency was assessed. As shown in Figures 1C and 1D, the expression of miR-4319 was significantly increased in HeLa and C33A cells transfected with miR-4319 mimic compared with NC mimic group. Collectively, miR-4319 was lowly expressed in CC tissues and cell lines.

3.2. Up-regulation of miR-4319 inhibits viability, and proliferation, and induces apoptosis of CC cells

Firstly, CCK-8 assay was adopted to evaluate the effects of miR-4319 on the viability of HeLa and C33A cells, and the data of Figure 2A displayed that miR-4319 mimic significantly inhibited the viability of HeLa and C33A cells in a time-dependent manner compared with NC mimic group. Besides, colony formation and EdU assays were carried out to assess the effects of miR-4319 on the proliferation of HeLa and C33A cells, and the data of Figures 2B and 2C showed that up-regulation of miR-4319 obviously suppressed the proliferation of HeLa and C33A cells compared with NC mimic group. Moreover, the effects of miR-4319 on the apoptosis of HeLa and C33A cells were determined by flow cytometry, and the data of Figure 2D indicated that compared with NC mimic group, over-expression of miR-4319 remarkably promoted the apoptosis of HeLa and C33 cells. Furthermore, western blot was performed to evaluate the effects of miR-4319 on the expression levels of apoptosis-related proteins including Bax, Bcl-2, Cleaved-caspase-3, and Cleaved-caspase-9 in HeLa and C33A cells. The data of Figure 2E showed that relative to NC mimic group, miR-4319 mimic notably reduced the protein expression of Bcl-2, but promoted the protein levels of Bax, Cleaved-caspase-3, and Cleaved-caspase-9 both in HeLa and C33A cells. These

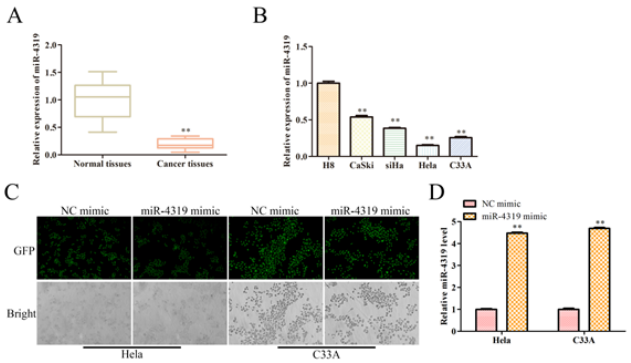

Fig. 1. miR-4319 is down-regulated in clinical tissues and cell lines. The expression of miR-4319in (A) CC tissues and (B) cell lines was detected by qRT-PCR assay. $^{**}P < 0.01$ vs. Normal tissues or H8 cells. (C) GFP and (D) qRT-PCR assays were performed to evaluate the miR-4319 expression in HeLa and C33A cells after transfection with miR-4319 mimic. $^{*}P < 0.05$, $^{**}P < 0.01$ vs. NC mimic. All data were presented as mean ± SD (n = 3).

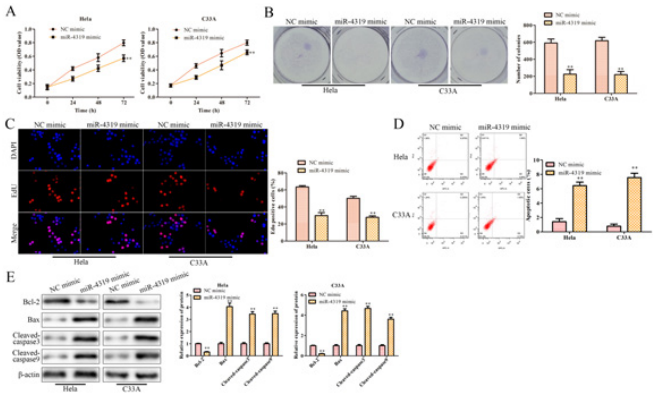

Fig. 2. Up-regulation of miR-4319 inhibits viability, proliferation, and induces apoptosis of CC cells. (A) The viability of HeLa and C33A cells transfected with miR-4319 mimic was assessed by CCK-8 assay at indicated times. The proliferation of HeLa and C33A cells transfected with miR-4319 mimic was evaluated by (B) colony formation and (C) EdU assays. (D) The apoptotic rate of HeLa and C33A cells transfected with miR-4319 mimic was determined by flow cytometry assay. (E) The expression levels of proteins, including Bax, Bcl-2, Cleaved-caspase-3, and Cleaved-caspase-9, were evaluated by western blot assay. $^{**}P < 0.01$ vs. NC mimic. All data were presented as mean ± SD (n = 3).

data suggested that up-regulation of miR-4319 inhibited viability, proliferation, and induced apoptosis of CC cells.

3.3. Up-regulation of miR-4319 inhibits migration and invasion of CC cells

Firstly, wound healing assay was performed to further explore the functional effects of miR-4319 on the migration of CC cells. As shown in Figure 3A, compared with the NC mimic group, miR-4319 mimic obviously inhibited the migration of HeLa and C33A cells. Then transwell migration and invasion assays were also carried out, and the data of Figure 3B suggested that compared with NC mimic group, over-expression of miR-4319 significantly inhibited the migration and invasion of HeLa and C33A cells. Furthermore, western blot was performed to evaluate the effects of miR-4319 on the expression levels of metastasis-related proteins, including Cox-2, MMP-2, and MMP-9. The data of Figure 3C revealed that relative to NC mimic group, miR-4319 mimic notably decreased the protein expressions of Cox-2, MMP-2, and MMP-9 in HeLa and C33A cells. These data suggested that up-regulation of miR-4319 inhibited migration and invasion of CC cells.

3.4. TUFT1 is direct target gene of miR-4319, and negatively associated with miR-4319

In order to study on the possible target genes of miR-4319 involved in the occurrence of CC, firstly, TargetScan (https://www.targetscan.org/vert_72/) was carried out to predict the binding sites between miR-4319 and TUFT1, implied that TUFT1 was potential candidate of miR-4319 (Figure 4A). TUFT1, as an important regulator, has been reported to control the occurrence and development of various tumors (20, 21). In addition, dual-luciferase reporter gene analysis was performed to verify whether miR-4319 directly regulated TUFT1, and the results of Figure 4B indicated that transfection with miR-4319 mimic significantly inhibited the activity of a firefly luciferase reporter containing wild-type TUFT1 3'-UTR, while had no effect on the activity of the mutated TUFT1 3'-UTR. The data suggested that TUFT1 was a direct target of miR-4319. To further confirm the targeting relationship between miR-4319 and TUFT1, qRT-PCR and western blot assays were used to determine the mRNA and protein expressions of TUFT1 in HeLa and C33A cells transfected with miR-4319 mimic. The data of Figure 4C and 4D showed that compared with NC mimic group, the mRNA and protein

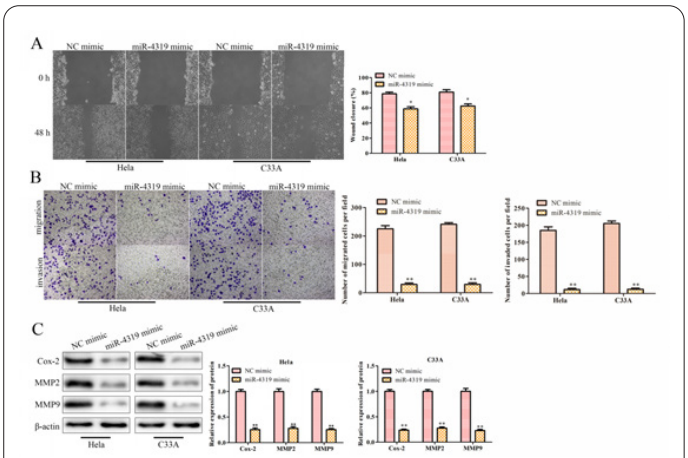

Fig. 3. Up-regulation of miR-4319 inhibits migration and invasion of CC cells. (A) The migration of HeLa and C33A cells transfected with miR-4319 mimic was determined by wounding healing assay. (B) The migration and invasion of HeLa and C33A cells transfected with miR-4319mimic were determined by transwell migration and invasion assays. (C) The expression levels of proteins, including Cox-2, MMP-2 and MMP-9, were evaluated by western blot assay. $^{*}P < 0.05$, $^{**}P < 0.01$ vs. NC mimic. All data were presented as mean ± SD (n = 3).

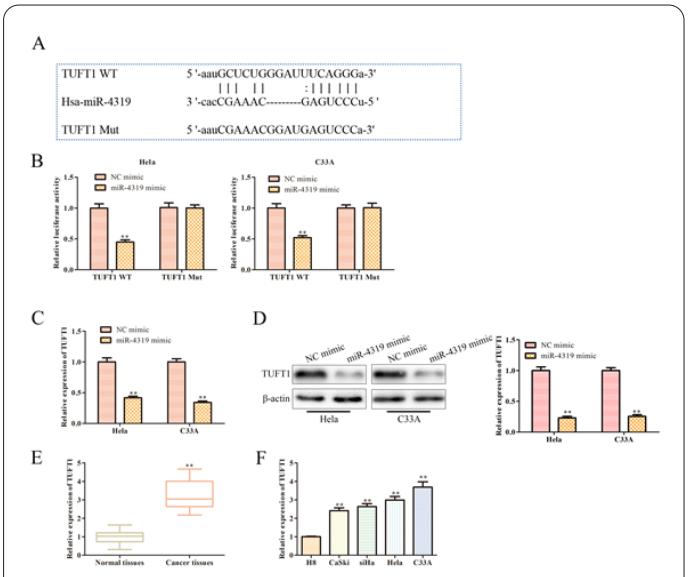

Fig. 4. TUFT1 is direct target gene of miR-4319, and negatively associated with miR-4319. (A) The binding sites between miR-4319 and TUFT1. (B) Luciferase-reporter analysis was employed to validate the coactions between miR-4319 and TUFT1. (C) qRT-PCR assay was performed to evaluate the TUFT1 expression in HeLa and C33A cells transfected with miR-4319 mimic. (D) Western blot assay was performed to evaluate the TUFT1 expression in HeLa and C33A cells transfected with miR-4319 mimic. $^{**}P < 0.01$ vs. NC mimic. The expression of TUFT1 in (E) CC tissues and (F) cell lines was detected by qRT-PCR assay. $^{**}P < 0.01$ vs. Normal tissues or H8 cells. All data were presented as mean ± SD (n = 3).

expression levels of TUFT1 were obviously down-regulated in HeLa and C33A cells transfected with miR-4319 mimic. Moreover, qRT-PCR assay was carried out to assess the TUFT1 in clinical CC tissues and CC cell lines, and the data of Figure 4E and 4F illustrated that TUFT1 was obviously up-regulated in clinical CC cancer tissues and CC cell lines. These data suggested that TUFT1 was direct target gene of miR-4319, and was negatively associated with miR-4319 in CC.

3.5. Up-regulation of miR-4319 inhibits viability, proliferation, migration and invasion, and induced apoptosis of CC cells via targeting TUFT1

Pc-TUFT1 was transfected into HeLa and C33A cells, and qRT-PCR was performed so as to explore whether miR-4319 functioned as a tumor suppressor gene through targeting TUFT1. The data of Figure 5A showed that after transfection with pc-TUFT1, the expression of TUFT1 was obviously increased in HeLa and C33A cells. Then, CCK-8 was performed to evaluate the effects of miR-4319/TUFT1 axis on the viability of HeLa and C33A cells. As shown in Figure 5B, up-regulation of TUFT1 obviously restored the inhibitory effects of miR-4319 mimic on the viability of HeLa and C33A cells. Besides, EdU assay showed that over-expression of TUFT1 obviously retarded the inhibitory effects of miR-4319 mimic on the proliferation of HeLa and C33A cells (Figure 5C). In addition, the results of Figure 5D indicated that up-regulation of TUFT1 obviously inhibited promoting effects of miR-4319 mimic on the apoptosis of HeLa and C33A cells. Furthermore, transwell migration and invasion results displayed that the up-regulation of TUFT1 obviously antagonized the inhibitory effects of miR-4319 mimic on the migration and invasion of HeLa and C33A cells. These data suggested that up-regulation of miR-4319 inhibited viability, proliferation, migration, and invasion, and induced apoptosis of CC cells via targeting TUFT1.

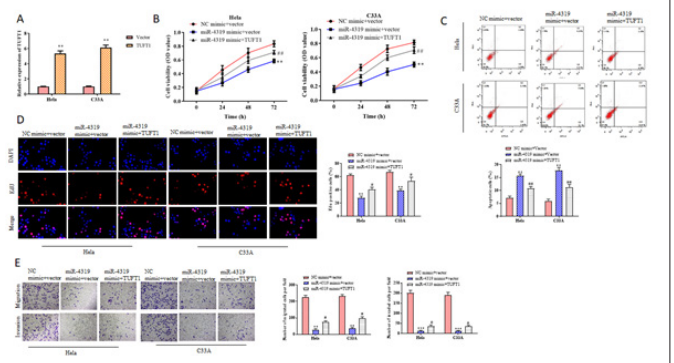

Fig. 5. Up-regulation of miR-4319 inhibits viability, proliferation, migration and invasion, and induced apoptosis of CC cells via targeting TUFT1. (A) The expression of TUFT1 in HeLa and C33A cells transfected with pc-TUFT1 was evaluated by qRT-PCR assay. $^{**}P < 0.01$ vs. Vector. (B) The viability of HeLa and C33A cells transfected with pc-TUFT1 was assessed by CCK-8 assay at indicated times. (C) The proliferation of HeLa and C33A cells transfected with pc-TUFT1 was evaluated by EdU assay. (D) The apoptotic rate of HeLa and C33A cells transfected with pc-TUFT1 was determined by flow cytometry assay. (E) The migration and invasion of HeLa and C33A9 cells transfected with pc-TUFT1 were determined by Transwell migration and invasion assays. $^{**}P < 0.01$ vs. NC mimic + vector. $^{\#}P < 0.05$, $^{\#\#}P < 0.01$ vs. miR-4319 mimic + vector. All data were presented as mean ± SD (n = 3).

4. Discussion

The etiology of CC involves complex molecular mechanisms, including activation of oncogenes and inhibition of tumor suppressor genes (22). With the continuous research on the molecular mechanisms of CC, more and more genes and proteins involved in the occurrence of CC have been reported, which promotes the diversity of treatment methods for CC, including gene-targeted therapy, hormone therapy and so on (23-25). In view of this, to explore the molecular mechanisms of the occurrence, metastasis and recurrence of CC, to find markers for clinical diagnosis and prognosis of CC, and to identify effective molecular targets have become the research hotspot of medical personnel in various countries. In view of the extensive existence of miRNAs and the diversity of gene regulation, much more attention has been paid to the role of miRNAs in the development and tumorigenesis in recent years (26-28). Among them, miR-4319 has been confirmed as a regulatory factor of gene mRNA transcription, regulating the post-transcriptional expression of specific target genes, and then participating in the pathological process of many cancers (29-31). However, the expression of miR-4319 in human CC and its biological mechanisms remained unclear.

It has been confirmed that miR-4319 is involved in the pathological process of many diseases, and is recognized as a tumor suppressor gene, which can be used as an independent factor of clinical prognosis of many cancers. For example, miR-4319 acts as a tumor suppressor in non-small cell lung cancer (NSCLC) progression via restraining cell proliferation and migration as well as boosting apoptosis through inhibiting LIN28-mediated RFX5 stability (32). MiR-4319 is notably down-regulated in thyroid cancer tissues and cells. Up-regulation of miR-4319 attenuates proliferation, migration, and epithelial-to-mesenchymal transition (EMT) in thyroid cancer via targeting SMURF1 (33). Moreover, miR-4319 level is decreased in prostate cancer (PC) specimens, and re-expression of miR-4319 in PC cells inhibits Her-2-dependent cell growth (34). Similarly, our study displayed that miR-4319 was low-expressed in CC tissues and cell lines. Up-regulation of miR-4319 repressed viability, proliferation, migration, invasion, and induced apoptosis of CC cells, suggesting that miR-4319 was an inhibitory factor of CC, which might participate in the occurrence and development of CC.

MiRNAs produce a marked effect through inducing mRNA degradation or translation inhibition by base pairing with 3'-UTR of target genes (35, 36). At present, post transcriptional regulation mechanisms of miRNAs on target genes play an important role in tumor development including CC (37-39). In this study, TUGT1 was highly expressed in CC tissues and cell lines. TUGT1 was predicted as a candidate target of miR-4319 by TargetScan, which was further confirmed by dual-luciferase reporter assay. TUFT1 gene is identified, cloned, and sequenced from ameloblast cDNA library by Deutsch et al (40, 41). TUFT1 is located at 1dq21.3, which is involved in the growth and maturation of extracellular enamel (41). At present, studies have focused on its relationship with enamel mineralization and tooth development. However, TUFT1 exists in many tissues, such as kidney, adrenal gland, liver, and testis (42). Furthermore, recent studies

have shown that TUFT1 is abnormally expressed in many kinds of tumors, and is closely related to the development of multiple tumors. TUFT1 is over-expressed in pancreatic cancer (PC), and depletion or over-expression of TUFT1 correspondingly inhibits or promotes PC cell migration and metastasis in vitro and in vivo, through regulation of EMT (20). TUFT1 is elevated in hepatocellular carcinoma (HCC), and promotes HCC cell growth, metastasis, and EMT in vitro and in vivo via activation of Ca^{2+}/PI3K/AKT pathway (21). TUFT1 expression is increased in breast cancer samples. Inhibition of TUFT1 expression in T-47D and MDA-MB-231 breast cancer cells significantly affects cell proliferation, induces apoptosis, and leads to G1-phase cell cycle arrest (41). These findings were closely in line with our studies. Through rescue experiments, over-expression of TUFT1 partially restored the effects of miR-4319 mimic on viability, proliferation, migration, and invasion of CC cells.

There are some limitations in our study. Firstly, it has been reported that TUFT1 affects tumor progression via regulating many signaling pathways, such as PI3K/AKT pathway and Rac1/β-catenin pathway (43, 44). However, whether miR-4319/TUFT1 axis is involved in CC progression through regulation of certain pathways remains unclear. In addition, the prognostic value of miR-4319 and TUFT1 in CC patients was not investigated. Therefore, further studies should be carried out to perfect our study in the future.

In conclusion, the expression of miR-4319 was decreased, while the expression of TUFT1 was increased in clinical CC tissues and cell lines. Up-regulation of miR-4319 inhibited the growth and metastasis of CC cells via targeting TUFT1, which provided research basis for gene-targeted therapy of CC in the future.

Informed consent
The authors report no conflict of interest.

Availability of data and material
We declared that we embedded all data in the manuscript.

Authors' contributions
ZL and RQ conducted the experiments and wrote the paper; ZW and TX analyzed and organized the data; GL conceived, designed the study and revised the manuscript.

Funding
This work was supported by Jiangsu Provincial Commission of Health and Family Planning (Grant No. QNRC2016881, F201922) and Suzhou Science and Technology Agency (Grant No. SYSD2019106).

Acknowledgements
We thanked The Second Affiliated Hospital of Soochow University approval our study.

Originality statement
This study was pre-printed by Research Square (https://www.researchsquare.com/article/rs-556240/v1). All authors confirm that the work described is original research that has not been published previously, and not under consideration for publication elsewhere, in whole or in part.

References

1. C. Zhang et al., The direct and indirect association of cervical microbiota with the risk of cervical intraepithelial neoplasia. Cancer Med 7, 2172 (2018).
2. N. C. Nkfusai et al., Cervical cancer in the Bamenda Regional Hospital, North West Region of Cameroon: a retrospective study. Pan Afr Med J 32, 90 (2019).
3. M. Saeed et al., A Synopsis on the Role of Human Papilloma Virus Infection in Cervical Cancer. Curr Drug Metab 19, 798 (2018).
4. M. Wei et al., Rising Mortality Rate of Cervical Cancer in Younger Women in Urban China. J Gen Intern Med 34, 281 (2019).
5. Z. Hu, D. Ma, The precision prevention and therapy of HPV-related cervical cancer: new concepts and clinical implications. Cancer Med 7, 5217 (2018).
6. A. E. Rizzo, S. Feldman, Update on primary HPV screening for cervical cancer prevention. Curr Probl Cancer 42, 507 (2018).
7. Mayadev JS et al., Global challenges of radiotherapy for the treatment of locally advanced cervical cancer. Int J Gynecol Cancer32, 436 (2022).
8. A. Dueñas-González, S. Campbell, Global strategies for the treatment of early-stage and advanced cervical cancer. Curr Opin Obstet Gynecol 28, 11 (2016).
9. Bedell SL, Goldstein LS, Goldstein AR, Goldstein AT. Cervical Cancer Screening: Past, Present, and Future. Sex Med Rev8, 28 (2020).
10. J. Hayes, P. P. Peruzzi, S. Lawler, MicroRNAs in cancer: biomarkers, functions and therapy. Trends Mol Med 20, 460 (2014).
11. K. Van Roosbroeck, G. A. Calin, Cancer Hallmarks and MicroRNAs: The Therapeutic Connection. Adv Cancer Res 135, 119 (2017).
12. B. Mansoori, A. Mohammadi, S. Shirjang, B. Baradaran, MicroRNAs in the Diagnosis and Treatment of Cancer. Immunol Invest 46, 880 (2017).
13. S. Park et al., MiR-9, miR-21, and miR-155 as potential biomarkers for HPV positive and negative cervical cancer. BMC Cancer 17, 017 (2017).
14. J. G. P. Sanches et al., miR-501 is upregulated in cervical cancer and promotes cell proliferation, migration and invasion by targeting CYLD. Chem Biol Interact 285, 85 (2018).
15. J. Chen, G. Li, MiR-1284 enhances sensitivity of cervical cancer cells to cisplatin via downregulating HMGB1. Biomed Pharmacother 107, 997 (2018).
16. M. Yang et al., Long noncoding RNA ITGB2-AS1 promotes growth and metastasis through miR-4319/RAF1 axis in pancreatic ductal adenocarcinoma. J Cell Physiol 20, 29471 (2020).
17. L. Huang et al., MiR-4319 suppresses colorectal cancer progression by targeting ABTB1. United European Gastroenterol J 7, 517 (2019).
18. J. Chu et al., MiR-4319 Suppress the Malignancy of Triple-Negative Breast Cancer by Regulating Self-Renewal and Tumorigenesis of Stem Cells. Cell Physiol Biochem 48, 593 (2018).
19. X. Hu et al., miR-4319 Suppresses the Growth of Esophageal Squamous Cell Carcinoma Via Targeting NLRC5. Curr Mol Pharmacol 13, 144 (2020).
20. B. Zhou et al., TUFT1 regulates metastasis of pancreatic cancer through HIF1-Snail pathway induced epithelial-mesenchymal transition. Cancer Lett 382, 11 (2016).
21. C. Dou et al., Hypoxia-induced TUFT1 promotes the growth and metastasis of hepatocellular carcinoma by activating the Ca(2+)/PI3K/AKT pathway. Oncogene 38, 1239 (2019).
22. P. Tsikouras et al., Cervical cancer: screening, diagnosis and staging. J Buon 21, 320 (2016).
23. H. Li, X. Wu, X. Cheng, Advances in diagnosis and treatment of

metastatic cervical cancer. J Gynecol Oncol 27, e43 (2016).
24. G. Menderes, J. Black, C. L. Schwab, A. D. Santin, Immunotherapy and targeted therapy for cervical cancer: an update. Expert Rev Anticancer Ther 16, 83 (2016).
25. S. Y. Brucker, U. A. Ulrich, Surgical Treatment of Early-Stage Cervical Cancer. Oncol Res Treat 39, 508 (2016).
26. V. Laengsri, U. Kerdpin, C. Plabplueng, L. Treeratanapiboon, P. Nuchnoi, Cervical Cancer Markers: Epigenetics and microRNAs. Lab Med 49, 97 (2018).
27. B. Pardini et al., MicroRNAs as markers of progression in cervical cancer: a systematic review. BMC Cancer 18, 018 (2018).
28. A. J. Granados-López et al., Use of Mature miRNA Strand Selection in miRNAs Families in Cervical Cancer Development. Int J Mol Sci 18, 407 (2017).
29. S. Han et al., MiR-4319 induced an inhibition of epithelial-mesenchymal transition and prevented cancer stemness of HCC through targeting FOXQ1. Int J Biol Sci 15, 2936 (2019).
30. F. Albano et al., SETBP1 and miR_4319 dysregulation in primary myelofibrosis progression to acute myeloid leukemia. J Hematol Oncol 5, 48 (2012).
31. Y. Wang, H. Zhao, W. Zhi, SEMA4D under the posttranscriptional regulation of HuR and miR-4319 boosts cancer progression in esophageal squamous cell carcinoma. Cancer Biol Ther 21, 122 (2020).
32. Y. Yang et al., MiR-4319 hinders YAP expression to restrain non-small cell lung cancer growth through regulation of LIN28-mediated RFX5 stability. Biomed Pharmacother 115, 14 (2019).
33. S. Bian, miR-4319 inhibited the development of thyroid cancer by modulating FUS-stabilized SMURF1. J Cell Biochem 121, 174 (2020).
34. X. Lin, Y. Wang, Re-expression of microRNA-4319 inhibits growth of prostate cancer via Her-2 suppression. Clin Transl Oncol 20, 1400 (2018).
35. J. Wu, Y. Zhao, F. Li, B. Qiao, MiR-144-3p: a novel tumor suppressor targeting MAPK6 in cervical cancer. J Physiol Biochem 75, 143 (2019).
36. H. Xiao et al., MiR-340 suppresses the metastasis by targeting EphA3 in cervical cancer. Cell Biol Int 42, 1115 (2018).
37. N. Li, T. Cui, W. Guo, D. Wang, L. Mao, MiR-155-5p accelerates the metastasis of cervical cancer cell via targeting TP53INP1. Onco Targets Ther 12, 3181 (2019).
38. Q. Hu et al., miR-146a promotes cervical cancer cell viability via targeting IRAK1 and TRAF6. Oncol Rep 39, 3015 (2018).
39. Q. Li, X. Yu, L. Yang, MiR-145 inhibits cervical cancer progression and metastasis by targeting WNT2B by Wnt/β-catenin pathway. Int J Clin Exp Pathol 12, 3740 (2019).
40. Y. Leiser et al., The induction of tuftelin expression in PC12 cell line during hypoxia and NGF-induced differentiation. J Cell Physiol 226, 165 (2011).
41. W. Liu et al., TUFT1 is expressed in breast cancer and involved in cancer cell proliferation and survival. Oncotarget 8, 74962 (2017).
42. D. Deutsch et al., The human tuftelin gene and the expression of tuftelin in mineralizing and nonmineralizing tissues. Connect Tissue Res 43, 425 (2002).
43. Yang Y et al., TUFT1 Facilitates Metastasis, Stemness, and Vincristine Resistance in Colorectal Cancer via Activation of PI3K/AKT Pathway. Biochem Genet59, 1018 (2021).44.
44. Liu W et al., TUFT1 Promotes Triple Negative Breast Cancer Metastasis, Stemness, and Chemoresistance by Up-Regulating the Rac1/β-Catenin Pathway. Front Oncol9, 9 (2019).